Int J Clin Exp Med 2018;11(2):1260-1269
www.ijcem.com /ISSN:1940-5901/IJCEM0059795

Original Article

Dysfunctional subpathways of osteoarthritis identified through combining lncRNA-mRNA expression profile with pathway topologies

An-Li Zhu, Meng-Po Fan, De-Qiang Liu

Department of Orthopaedic Trauma, The Second People's Hospital of Liaocheng, Linqing 252600, Shandong, China

Received June 19, 2017; Accepted December 7, 2017; Epub February 15, 2018; Published February 28, 2018

Abstract: Objective: Concept of key local subregion is more meaningful for revealing the pathogenesis of diseases, relative to entire pathways. Thus, in our study, we planned to use the subpathway strategy to extract altered subpathways competitively regulated by lncRNAs involved in osteoarthritis (OA) through lncRNA-mRNA expression profile and pathway topologies. Methods: Candidate lncRNA-mRNA interactions were constructed and reweighted using PCC. Using KEGG pathways as backbone, undirected graphs were displayed where genes were as nodes and regulated relations stood for edges. Condition-specific lncRNA competitively regulated signal pathways (LRSP) were inferred. Subsequently, interesting lncRNAs and genes were aligned to LRSP, and then subpahtways were detected using "lenient distance" similarity method. Eventually, we evaluated the significance of candidate subpathways through Wallenius approximation, following by identification of hub lncRNAs in the LRSP. Results: After reweighting using PCC, 54 lncRNAs, 130 mRNAs and 147 co-expressed interactions were detected. Then, 31 seed pathways were identified after these 130 mRNAs were mapped to the reference pathways. we transformed seed pathways into undirected graphs, and the 54 lncRNAs were embedded into pathway graphs to establish the condition-specific LRSP. Overall 35 significant lncRNAs competitively regulating subpathways involved in 24 complete pathways were identified in the LRSP. The top three subpathways included cell cycle, PI3K-Akt signaling pathway, and focal adhesion. There were 4 hub lncRNAs, including SLC38A3, LINC00242, DCP1A, and EPB41L4A-AS1. Conclusions: The strategy of subpathways is feasible to predict marker pathways for OA. Subpathways of cell cycle, PI3K-Akt signaling pathway, and focal adhesion might play crucial roles in OA progression.

Keywords: Osteoarthritis, subpathway, long noncoding RNAs

Introduction

Osteoarthritis (OA), as one of the most prevalent chronic, and age-related degenerative joint disorder, is characterized by degradation of articular cartilage along with pain and disability [1, 2]. More than 50% of patients with symptomatic OA are younger than 65 years old [3]. Unfortunately, OA is becoming a primary health problem in China in view of the increasing life expectancy of the population. Therapy strategies to slow down the OA progression remain still limited, and the damage is irreversible at the time of diagnosis. Together, this emphasizes the importance to increase insight into the disease causes and to optimize therapeutic approaches as well as develop novel therapeutic drugs.

OA is considered as a multifactorial disease. In addition to joint instability, aging and obesity, genetic links to OA susceptibility have been found in several studies [4, 5]. Epigenetic effects, especially noncoding RNAs, likely contribute to the onset and progression of OA [6]. Noncoding RNAs (ncRNAs) have emerged as a new identified class of RNA molecules without protein-coding capacity [7]. Based on their size, ncRNAs include two main categories: small ncRNAs, and long ncRNAs (lncRNAs) [8]. It has been reported that lncRNA play crucial roles in various key biological processes [9, 10], for example, posttranscriptional regulation [11] and human disease [12]. Significantly, lncRNAs have been indicated to exert important functions in the processes of bone and cartilage development [13]. Growing evidence has impli-

cated that lncRNAs competitively regulate mRNAs expression through sharing common miRNA binding sites with mRNAs [14, 15]. Zhang et al. [16] have suggested that lncRNA UFC1 may play important roles as a endogenous miRNA-34a sponge to promote the proliferation of OA chondrocyte. Moreover, a former study provided by Song et al. demonstrated that a lncRNA GAS5 contributed to the pathogenesis of OA via serving as a negative regulator of miRNA-21 [17]. Further, a previous study has indicated that lncRNA CIR plays a crucial role in the pathogenesis of OA via contributing to the degradation of chondrocyte extracellular matrix [18]. Since the RNA competitive interaction could influence biological functions in disease, extracting lncRNA competitively regulated pathways not only shed new insights into the pathogenic processes, but also is beneficial for uncovering the cellular functions of lncRNAs in disease. On the contrary, few methods are able to systematically track dysfunctional pathways which are competitively mediated by lncRNAs in disease states. Additionally, paying more attention on subpathways instead of entire pathways might extract more biologically meaningful pathways and dissect the functional roles of lncRNAs. Excitedly, Shi et al. [19] proposed the concept of key local subregion which is more meaningful for revealing the molecular mechanisms of diseases relative to the entire pathways.

Consequently, in the current work, we aimed to identify the lncRNAs competitively regulated signal subpathways in OA using the subpathway strategy based on lncRNA-mRNA expression profile and pathway topologies. We confirm that this novel method can provide a flexible tool to extract lncRNA competitively regulated subpathways in OA, and is beneficial for expounding the functional roles of lncRNAs in OA.

Materials and methods

Proposed protocol

In the present analysis, using KEGG pathways as backbone, undirected graphs were displayed where genes were as nodes and regulated relations stood for edges. Next, condition-specific lncRNA competitively regulated signal pathways (LRSP) were inferred according to the matched lncRNA-mRNA expression data as well as the common miRNAs. Subsequently, interesting lncRNAs and genes were aligned to LRSP, and then subpahtways were located in pathways based on the "lenient distance" similarity method [19]. Eventually, we evaluated the significance of candidate subpathways by means of Wallenius approximation [20], following by the identification of hub lncRNAs in the LRSP.

Microarray data about OA

Gene expression profile from OA cartilage were collected from Gene Expression Omnibus (GEO) database (Access ID: GSE57218) [21] based on the GPL6947 platform of Illumina HumanHT-12 V3.0 expression beadchip. In the GSE57218, there were 7 healthy samples, 33 OA samples, and 33 OA preserved cartilage samples. In order to better reveal the molecular mechanisms of OA, we only selected 7 healthy samples and 33 OA samples for further analysis. After probes were aligned to the gene symbols, a total of 19,293 genes were obtained.

Constructing candidate lncRNA-mRNA interaction

LncRNA-related competing triplets (lncRNA-miRNA-mRNA interactions) were firstly collected. Specifically, the lncRNA-miRNA interactions were downloaded from StarBase version 2.0 [22], and mRNA-miRNA interactions were obtained from mirTarBase, TarBase, miRecords (V4.0), and mir2Disease. Next, according to the shared miRNAs, candidate lncRNA-mRNA competitively regulated relationships were constructed. For each lncRNA, we identified its candidate competing mRNAs when they met the following two criteria: first, hypergeometric test of common miRNAs under false discovery rate (FDR) < 0.05; second, Jaccard Coefficient of lncRNA-mRNA intersections ranked at top 20%. With the goal of ensuring the reliability of data, the interactions which fulfilled both conditions were reserved. Eventually, candidate lncRNA-mRNA competitively regulated interactions covered 7693 lncRNAs-mRNA interactions among 1749 genes and 835 lncRNAs. Then, the intersection between 19,293 genes and 7693 lncRNAs-mRNA interactions was taken, and finally, we obtained 1690 mRNAs and 116 lncRNAs.

Reweighting the lncRNAs-mRNA interactions using Pearson correlation coefficient (PCC)

To the best of my knowledge, PCC is a measure about correlation between two variables,

Table 1. List of seed pathways based on false discovery rate (FDR) < 0.01

Pathways	FDR
Prostate cancer	4.25E-11
Cell cycle	5.82E-10
Pathways in cancer	3.49E-08
PI3K-Akt signaling pathway	5.02E-08
Glioma	2.24E-06
Small cell lung cancer	3.08E-06
Hepatitis B	6.45E-05
Focal adhesion	9.17E-05
p53 signaling pathway	2.17E-04
Endometrial cancer	3.32E-04
Adherens junction	3.38E-04
Basal cell carcinoma	4.52E-04
HIF-1 signaling pathway	5.42E-04
ErbB signaling pathway	9.83E-04
GnRH signaling pathway	1.37E-03
Neurotrophin signaling pathway	1.48E-03
Amyotrophic lateral sclerosis (ALS)	2.22E-03
Melanogenesis	2.35E-03
Non-small cell lung cancer	3.37E-03
Epstein-Barr virus infection	3.66E-03
DNA replication	3.94E-03
Viral carcinogenesis	4.20E-03
Hypertrophic cardiomyopathy (HCM)	4.38E-03
Oocyte meiosis	4.40E-03
Bladder cancer	4.79E-03
Transcriptional misregulation in cancers	5.21E-03
Dilated cardiomyopathy (DCM)	5.79E-03
Herpes simplex infection	6.45E-03
Pancreatic cancer	6.82E-03
Olfactory transduction	6.82E-03
Melanoma	9.24E-03

whose range is from -1 to 1 [23]. In our study, PCC was utilized to measure the co-expression possibility for any pair of relations in the candidate lncRNA-mRNA interactions on the basis of matched lncRNA and mRNA expression profiles. Using Fisher's Z transform [24], those r value had reached a significant positive threshold were retained ($P < 0.05$).

Reconstructing condition-specific LRSP

Identification of seed pathways: Kyoto Encyclopedia of Genes and Genomes (KEGG) is a database to provide a reference knowledge base for understanding cellular processes through pathway aligning, which means to map genes to KEGG reference pathways to infer systemic behaviors of cell [25]. In the current analysis, we recruited all the KEGG reference pathways from the database of KEGG. Then, we mapped mRNAs of the reweighted lncRNAs-mRNA interactions to the KEGG reference pathways to extract the seed pathways. The raw *P* values were corrected using FDR based on Benjamini-Hochberg method [26]. Seed pathways were detected when the FDR was set as 0.01.

Linking LncRNAs to regulated-mRNAs within pathway graphs: We transformed seed pathways into undirected graphs kept original pathway structural information by means of the developed R packages provided by Li et al. [27]. The lncRNAs in the reweighted lncRNAs-mRNA interactions were embedded into pathway graphs as nodes by connecting to their regulated-mRNAs. Finally, we obtained condition-specific LRSP, which covered lncRNA nodes and lncRNA-mRNA competitively regulated edges.

Locate subpathways competing regulated by lncRNAs: LncRNAs participating in the competing regulation and genes of interests were considered as signature nodes. These nodes combined with topology feature of LRSP can help us effectively locating lncRNA-regulated subregions. To begin with, we aligned signatures nodes to LRSP, then positing subpathways competing regulated by lncRNAs employed "lenient distance" similarity and network topology feature. Succinctly, the shortest path between any two signature nodes was calculated, if the count of molecules between each pair of signatures was no more than *n*, then we would merge them into one nodes. At the end, the count of nodes in the molecule sets in pathway no smaller than *s* were determined as candidate subpahtways competing regulated by lncRNAs. The *n* and *s* indexes respectively controlled the intensity of regulated signals and the size of candidate subpathways. In our study, $n = 1$ and $s = 8$ were used as default parameters.

Assessing the significance of candidate subathways: In order to assess whether the candidate subpathways were competing regulated by lncRNAs comparing random, Wallenius approximation methods was utilized to evaluate the significance of candidate subpathways,

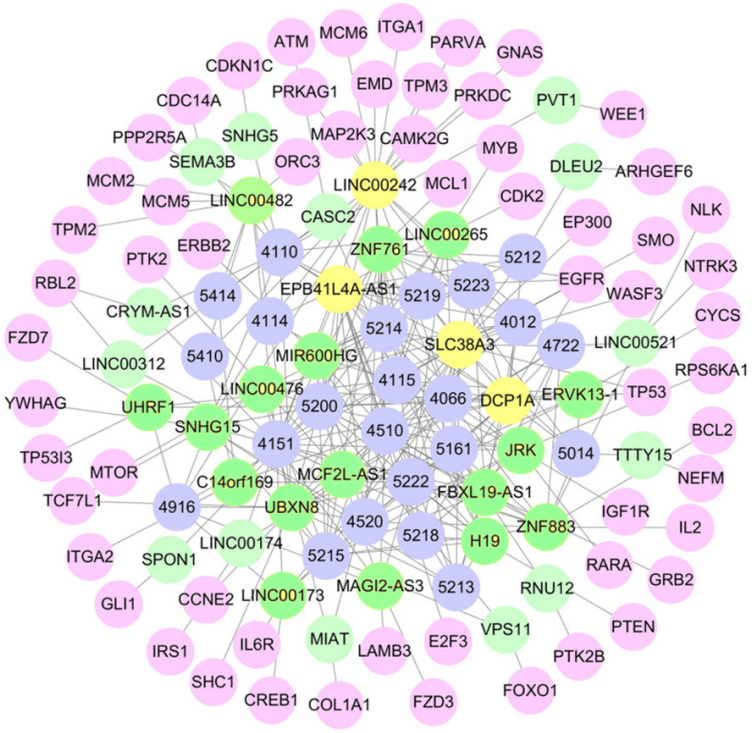

Figure 1. Osteoarthritis (OA)-relevant lncRNA competitively regulated signal subpathways network. Pink nodes represented mRNAs, and purple nodes denoted pathway IDs, green and yellow nodes stood for lncRNAs. Significantly, yellow nodes were on behalf of hub lncRNAs.

which was executed using R package BiasedUrn [28]. The following parameters were used: the count of interesting mRNAs (x); the count of background mRNAs (y); the count of background mRNAs enriched in this subpathways (m1); the count of interesting mRNAs involved in the given subpathway (m2); and the weight value of this subpathway (W). The weight parameter indicated the intensity of competing regulation by lncRNAs annotated into this given subpathway, which was calculated as follows:

$$W = 1 + \beta\left(-\log_2\left(\frac{G_L}{P_G}\right)\right)$$

In this equation, P_G was the number of mRNAs annotated into this subpathways, and G_L denoted the count of mRNAs competitively regulated by lncRNAs in this subpathway. β represented the parameter of control (herein, β = 1). The original *P* values were calculated based on the formula of *P*-values = F (x, m1, m2, y, $weight_i$). Then, the *P* values were adjusted using FDR. Finally, the significant subpathways with FDR < 0.01 were extracted in our study.

Dissecting hub lncRNAs in OA-relevant LRSP network

As we all kno, hub nodes were frequently very important in the biological network as whose connectivities were extremely high. Thus, we paid attention to the hub lncRNAs in the LRSP network. In our study, the top 10% of lncRNAs with the highest degrees in the network were selected and regarded as the hub lncRNAs.

Reproducibility and robustness analyses

To verify that the results obtained using subpathway strategy were reproducible, we used it to analyze a second OA data set GSE51588 including 20 OA samples and 5 nonOA samples.

In order to examine the stability of subpathway strategy, we evaluated its performance after randomly disturbing LRSP.

Statistical analysis

In our study, we used Feature Extraction software (version 10.7; Agilent Technologies, Inc., Santa Clara, CA, USA) to analyze the statistical significance of the microarray results. The FDR was computed to correct the original *P*-values. The threshold value used to designate the common miRNAs was FDR ≤ 0.05, and the cut-off criteria for significant subpathways was FDR < 0.01. P < 0.05 was regarded to indicate a statistically significant difference. In the present study, SPSS version 18.0 (SPSS, Inc., Chicago, IL, USA) was used for statistical analysis.

Results

Identification of co-expressed lncRNA-mRNA interactions and seed pathways

In our study, we used PCC to measure the co-expression possibility for any pair of relations in the candidate lncRNA-mRNA interactions on

Table 2. Subpathways extracted based on lncRNA-mRNA expression profile and pathway topologies

Pathway ID	Pathways	Molecule ratio (m2/x)	Bg ratio (m1/y)	Weight	FDR
04110_1	Cell cycle	13/135	20/26232	1.621488	4.28E-17
04151_2	PI3K-Akt signaling pathway	14/135	19/26232	1.440573	1.06E-16
04510_1	Focal adhesion	12/135	17/26232	1.502513	1.91E-16
05200_1	Pathways in cancer	21/135	29/26232	1.465664	1.95E-16
05214_1	Glioma	8/135	11/26232	1.459432	3.26E-16
05215_1	Prostate cancer	14/135	21/26232	1.584963	5.32E-15
04115_1	P53 signaling pathway	7/135	9/26232	1.362572	9.90E-15
04012_1	ErbB signaling pathway	6/135	8/26232	1.415037	1.01E-12
04066_1	HIF-1 signaling pathway	6/135	8/26232	1.415037	1.01E-12
04520_1	Adherens junction	6/135	8/26232	1.415037	1.01E-12
05414_1	Dilated cardiomyopathy	6/135	8/26232	1.415037	1.01E-12
05212_1	Pancreatic cancer	5/135	6/26232	1.263034	3.43E-11
05223_1	Non-small cell lung cancer	5/135	6/26232	1.263034	3.43E-11
05410_1	Hypertrophic cardiomyopathy (HCM)	5/135	6/26232	1.263034	3.43E-11
04151_4	PI3K-Akt signaling pathway	5/135	7/26232	1.485427	1.12E-10
04722_1	Neurotrophin signaling pathway	4/135	5/26232	1.321928	4.01E-09
05161_2	Hepatitis B	4/135	5/26232	1.321928	4.01E-09
05213_1	Endometrial cancer	4/135	5/26232	1.321928	4.01E-09
05218_1	Melanoma	4/135	5/26232	1.321928	4.01E-09
05219_1	Bladder cancer	4/135	5/26232	1.321928	4.01E-09
04114_2	Oocyte meiosis	4/135	6/26232	1.584963	1.04E-08
05014_1	Amyotrophic lateral sclerosis (ALS)	4/135	6/26232	1.584963	1.04E-08
05222_2	Small cell lung cancer	4/135	6/26232	1.584963	1.04E-08
04916_3	Melanogenesis	3/135	4/26232	1.415037	5.31E-07

the basis of matched lncRNA and mRNA expression profiles. Based on $P < 0.05$, we identified a total of 54 lncRNAs, 130 mRNAs and 147 co-expressed interactions (Supplementary Table 1). Then, we mapped these 130 mRNAs to the reference pathways to further detect the seed pathways. Ultimately, overall 31 seed pathways were identified when the FDR was set as less than 0.01 (**Table 1**).

Detecting signal subpathways competitively regulated by lncRNAs

After the seed pathways were identified, we transformed seed pathways into undirected graphs, and the 54 lncRNAs in the reweighted lncRNAs-mRNA interactions were embedded into pathway graphs as nodes by connecting to their regulated-mRNAs. Then, condition-specific LRSP was constructed, which covered lncRNA nodes and lncRNA-mRNA competitively regulated edges. Specific LRSP was shown in **Figure 1**. In this network, we found that overall 35 significant lncRNAs competitively regulating subpathways involved in 24 complete pathways with FDR < 0.01 (**Table 2**).

In further analysis, we focused on top three subpathways that competitively regulated by lncRNAs (**Figure 2**). The first is the most significant subpathway path: 04110_1, which was a subregion of cell cycle pathway (**Figure 2A**). Then, we further revealed this subpathway, and observed that this subregion was competitively regulated by 11 lncRNAs. Among these lncRNAs, LINC00482, directly regulated three genes (MCM2, MCM3, and ORC3). Moreover, MCM2 was coordinately regulated by two lncRNAs, LINC00265 and LINC00482.

The second significant subpathways was path: 04151-2, an important sub region in PI3K-Akt signaling pathway (**Figure 2B**). In this subpathway, TP53 gene encodes for a nuclear phosphoprotein of 53 kd (p53) participated in cell cycle control. Notably, this gene TP53 was coordinately regulated by two lncRNAs, DCP1A, and SLC38A3.

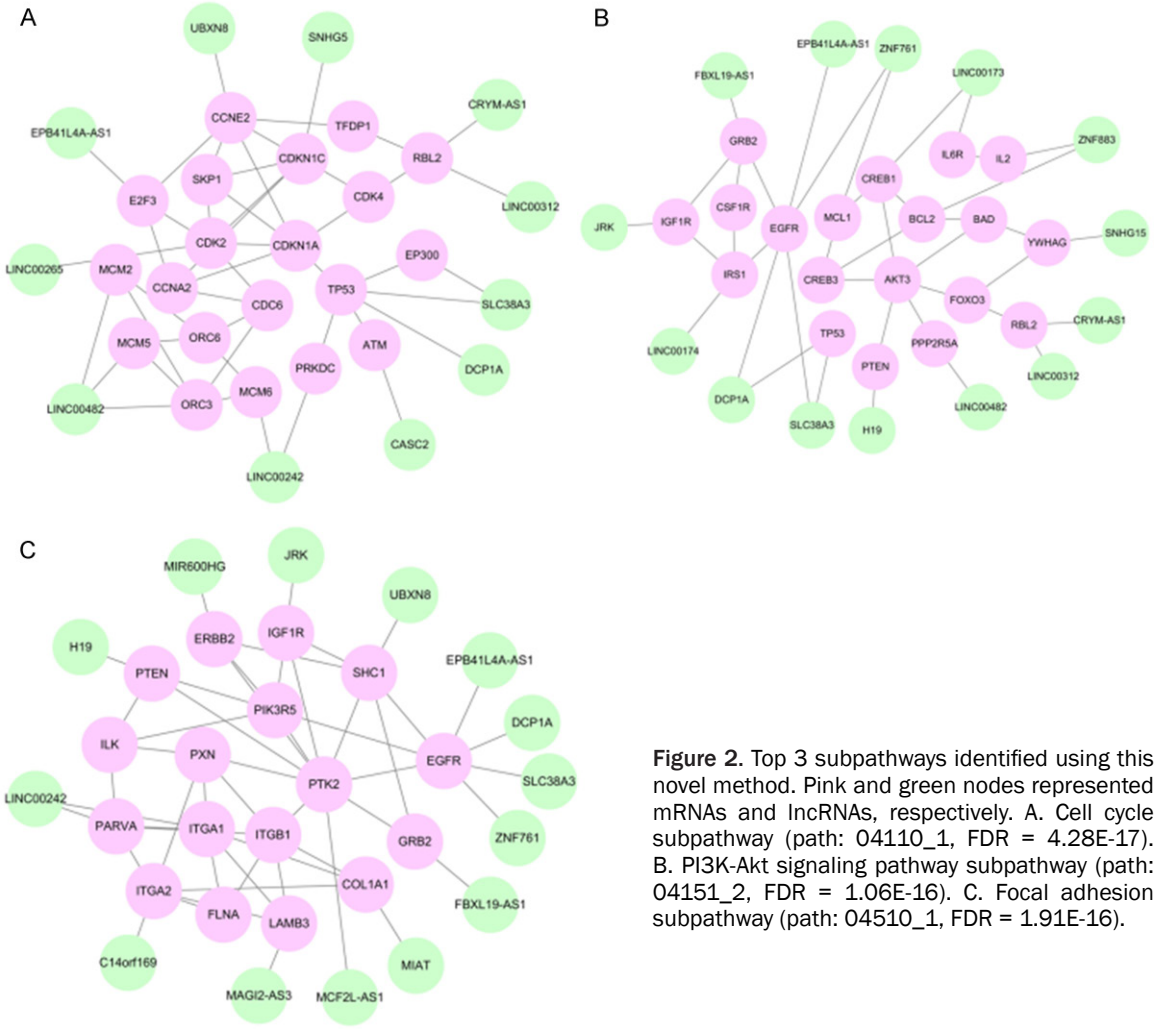

Figure 2. Top 3 subpathways identified using this novel method. Pink and green nodes represented mRNAs and lncRNAs, respectively. A. Cell cycle subpathway (path: 04110_1, FDR = 4.28E-17). B. PI3K-Akt signaling pathway subpathway (path: 04151_2, FDR = 1.06E-16). C. Focal adhesion subpathway (path: 04510_1, FDR = 1.91E-16).

The third subpathway, path: 04510_1, was a part of focal adhesion pathway (**Figure 2C**). Within this subpathway, EGFR was a growth-factor-receptor tyrosine kinase which was competitively regulated by four lncRNAs, DCP1A, SLC38A3, ZNF761 and EPB41LA-AS1. In a nutshell, these results demonstrated that this approach could identified biological meaningful subpathways, and highlighted some critical lncRNAs in OA condition.

Dissecting hub lncRNAs in OA-relevant LRSP network

In order to extract key lncRNAs associated with OA, we performed degree analysis for all nodes within the LRSP. Based on the degree distribution, we extracted 4 hub lncRNAs, including SLC38A3 (degree = 25), LINC00242 (degree = 23), DCP1A (degree = 21), and EPB41L4A-AS1 (degree = 18).

Reproducibility and robustness analyses

Reproducibility analysis: To prove that the results obtained using subpathway strategy were reproducible, we used this method to analyze another OA data set GSE51588 including 20 OA samples and 5 nonOA samples. A total of 19 significant subpathways involved in 19 complete pathways were identified from GSE51588 (FDR < 0.01). Among these 19 pathways, 12 pathways were identified by the two OA data sets, and 7 of these pathways undetected in GSE57218. This further suggested that the results obtained using subpathway strategy were reproducible.

Robustness analysis: To test the stability of subpathway strategy, we evaluated the performance of subpathway strategy through randomly removing a percentage of the edges in LRSP from 5% to 30% (N= 5, 10, ..., 30). This

deletion process repeated 100 times to receive 100 random LRSP lists. Subsequently, we conducted the subpathway method on OA data for each random LRSP list. When the deletion percentage increased, the recalled ratio of significant pathways declined slightly. Subpathway strategy showed that the best performance when the deleted percentage was 15%, recalling more than 91% of the pathways. Of note, the recalled ratio was 84%, as disturbing up to 25% edges within the LRSP, In a nutshell, these suggested that the subpathway strategy was robust.

Discussion

In recent years, studies suggests that lncRNAs can interact with miRNAs to further function as the miRNA decoy, thereby competitively affecting miRNA regulation of mRNAs as well as maintain normal biological functions [29, 30]. Thus, disruption of the biological functions competitively regulated by lncRNAs may cause the initiation of diseases, and thus, a better understanding of this regulation mechanism might provide new opportunities for developing novel target therapies. Nevertheless, so far, few methods were developed to identify the biological functions competitively regulated by lncRNAs and the functions of these lncRNAs have not be well expounded in disease conditions. Moreover, Shi et al. have demonstrated that paying more attention to key local subregions instead of complete pathways might be more significant in extraction of disease-associated pathway and might be more explainable to reveal the functional roles of lncRNAs in disease. In addition, this subregion method combining lncRNAmRNA expression profile with pathway topologies had several merits. To begin with, lncRNA representing a new regulatory layer were included in the pathway analysis. Second, it comprehensively analyzed the joint effect of lncRNAs, lncRNAs competitively regulated genes, and pathway topologies. Third, the method of subpathway might screen more biologically meaningful pathways. Thus, in our study, a subregion strategy was proposed to detect lncRNAs competitively regulated subpathways for OA, thereby to further explore the molecular mechanism underlying OA. Overall, we identified 35 significant lncRNAs competitively regulating subpathways involved in 24 complete pathways. We only focused on the top three different subpathways that competitively mediated by lncRNAs.

The first is the most significant subpathway path: 04110_1, which was a subregion of cell cycle pathway. Cell cycle has been demonstrated to influence the function of chondrocytes, which results in the division and duplication of chondrocytes. Cell proliferation would be blocked in inflammatory synovial tissue to arrest self-renewal and promote inflammation [31]. While, inflammation is a major contributing factor associated with the risk of cartilage loss and symptom progression in OA [32]. In addition, Yang and Wang have implicated that cell cycle as well as the related genes (CDK1 and MAD2L1), might play important roles in the development of OA [33]. Significantly, OA chondrocytes has a very low proliferative activity, and promoting chondrocyte proliferation through enhancing G2/M transition is a mechanism of treating OA [34]. Other studies also have demonstrated that promoting chondrocyte proliferation might be an efficient treatment to cure or delay the progression of OA [35, 36]. Accordingly, we further confirmed that cell cycle indeed contribute the initiation and progression of OA, these also proved that this strategy was an available method to reveal the OA pathogenesis.

The second significant subpathways was path: 04151-2, an important sub region in PI3K-Akt signaling pathway. Intracellular pathway PI3K/Akt has been reported to participate in extracellular matrix (ECM) alterations [37]. Fragments of ECM proteins (fibronectin and collagen) in turn, stimulate the generation of inflammatory cytokines, and chemokines [38]. ECM protein fragments has also been suggested to stimulate matrix destruction, and then ultimately resulting in cartilage degradation and contributing to the onset of OA [39]. More importantly, PI3K/Akt pathway might play key roles in the OA progression [40]. In this subpathway in our study, TP53 gene encodes for a nuclear phosphoprotein of 53 kd (p53) participated in cell cycle control, which exerts important functions in OA [41, 42]. Thus, we speculated that PI3K-Akt signaling subpathway exerted key functions in the occurrence and development of OA.

The third subpathway, path: 04510_1, was a part of focal adhesion pathway. Within this subpathway, EGFR was a growth-factor-receptor tyrosine kinase which was competitively regulated by four lncRNAs, DCP1A, SLC38A3,

ZNF761 and EPB41LA-AS1. EGFR is crucially important for cartilage matrix degradation in the period of endochondral ossification [43]. A previous study has reported that activation of EGFR signaling stimulates the expression of matrix metalloproteinases, resulting in increased cartilage matrix degradation by chondrocytes and osteoclasts at the chondro-osseous junctions in OA [44, 45]. Focal adhesions are specialized structures at the cellular-ECM contact points. Zintzaras et al. provided the evidence of functions of focal adhesion family genes in OA [46]. In a nutshell, these results demonstrated that this approach could identified biological meaningful subpathways in OA condition.

Notably, in our study, the lncRNA of SLC38A3 had the highest degree in the LRSP. Moreover, this hub lncRNA mediated the subpathways of PI3K-Akt signaling pathway and focal adhesion. SLC38A3 is also known as SNAT3, or SN1 [47]. SLC38A3, one member of System N subfamily, owns a preference for glutamine [48]. Moreover, SLC38A3 has been demonstrated to be involved in glutamate/γ-aminobutyric acid (GABA)-glutamine cycle and regulates the amount of glutamine [49]. Further, GABA levels have been indicated to be related to the chronic knee OA pain [50]. As we all know, no studies have reported the relationship between SLC38A3 and OA. Based on these results, we demonstrated that this lncRNA SLC38A3 might play important roles in OA progression.

Conclusion

In conclusion, a total of 35 significant lncRNAs competitively regulating subpathways involved in 24 complete pathways were successfully identified in our study. Based on the results, we indicated that the top 3 subpathways of cell cycle, PI3K-Akt signaling pathway, and focal adhesion were closely related to OA. Nevertheless, the confirmation by means of other datasets is needed to prove that these subpathways are helpful in distinguishing OA from normal samples.

Acknowledgements

This research received no specific grants from any funding agency in public, commercial, or not-for-profit sectors.

Disclosure of conflict of interest

None.

Address correspondence to: De-Qiang Liu, Department of Orthopaedic Trauma, The Second People's Hospital of Liaocheng, No. 306 Jiankang Street, Linqing 252600, Shandong, China. Fax: +86-0635-2342472; Tel: +86-0635-2342472; E-mail: liudqlq@163.com

References

[1] Moulton SG, Bhatia S, Civitarese DM, Frank RM, Dean CS and Laprade RF. Surgical techniques and outcomes of repairing meniscal radial tears: a systematic review. Arthroscopy 2016; 32: 1919-1925.

[2] Sacitharan PK and Vincent TL. Cellular ageing mechanisms in osteoarthritis. Mamm Genome 2016; 27: 421-429.

[3] Deshpande BR, Katz JN, Solomon DH, Yelin EH, Hunter DJ, Messier SP, Suter LG and Losina E. The number of persons with symptomatic knee osteoarthritis in the united states: impact of race/ethnicity, age, sex, and obesity. Arthritis Care Res (Hoboken) 2016; 68: 1743-1750.

[4] Pottie P, Presle N, Terlain B, Netter P, Mainard D and Berenbaum F. Obesity and osteoarthritis: more complex than predicted! Ann Rheum Dis 2006; 65: 1403.

[5] Livshits G, Kato BS, Zhai G, Hart DJ, Hunter D, Macgregor AJ, Williams FM and Spector TD. Genomewide linkage scan of hand osteoarthritis in female twin pairs showing replication of quantitative trait loci on chromosomes 2 and 19. Ann Rheum Dis 2007; 66: 623-627.

[6] Reynard LN and Loughlin J. Genetics and epigenetics of osteoarthritis. Maturitas 2012; 71: 200-204.

[7] Riquelme I, Ili C, Roa JC and Brebi P. Long noncoding RNAs in gastric cancer: mechanisms and potential applications. Oncotarget 2016.

[8] Brosnan CA and Voinnet O. The long and the short of noncoding RNAs. Curr Opin Cell Biol 2009; 21: 416-425.

[9] Wilusz JE, Sunwoo H and Spector DL. Long noncoding RNAs: functional surprises from the RNA world. Genes Dev 2009; 23: 1494-1504.

[10] Wang KC and Chang HY. Molecular mechanisms of long noncoding RNAs. Mol Cell 2011; 43: 904-914.

[11] Mercer TR, Dinger ME and Mattick JS. Long non-coding RNAs: insights into functions. Nat Rev Genet 2009; 10: 155-159.

[12] Barsytelovejoy D, Lau SK, Boutros PC, Khosravi F, Jurisica I, Andrulis IL, Tsao MS and Penn LZ. The c-Myc oncogene directly induces the H19 noncoding RNA by allele-specific binding to po-

tentiate tumorigenesis. Cancer Res 2006; 66: 5330-5337.
[13] Ponting CP, Oliver PL, Reik W. Evolution and functions of long noncoding RNAs. Cell 2009; 136: 629-641.
[14] Tay Y, Rinn J and Pandolfi PP. The multilayered complexity of ceRNA crosstalk and competition. Nature 2014; 505: 344.
[15] Ebert MS and Sharp PA. Emerging roles for natural microRNA sponges. Current Biology 2010; 20: R858.
[16] Zhang G, Wu Y, Xu D and Yan X. Long noncoding RNA UFC1 promotes proliferation of chondrocyte in osteoarthritis by acting as a sponge for miR-34a. DNA Cell Biol 2016; 35: 691-695.
[17] Song J, Ahn C, Chun CH and Jin EJ. A long noncoding RNA, GAS5, plays a critical role in the regulation of miR-21 during osteoarthritis. J Orthop Res 2014; 32: 1628-1635.
[18] Liu Q, Zhang X, Dai L, Hu X, Zhu J, Li L, Zhou C and Ao Y. Long noncoding RNA related to cartilage injury promotes chondrocyte extracellular matrix degradation in osteoarthritis. Arthritis Rheumatol 2014; 66: 969-978.
[19] Shi X, Xu Y, Zhang C, Feng L, Sun Z, Han J, Su F, Zhang Y, Li C, Li X. Subpathway-LNCE: Identify dysfunctional subpathways competitively regulated by lncRNAs through integrating lncRNA-mRNA expression profile and pathway topologies. Oncotarget 2016; 7: 69857-69870.
[20] Epstein MP, Duncan R, Jiang Y, Conneely KN, Allen AS and Satten GA. A permutation procedure to correct for confounders in case-control studies, including tests of rare variation. Am J Hum Genet 2012; 91: 215.
[21] Ramos YF, den Hollander W, Bovée JV, Bomer N, van der Breggen R, Lakenberg N, Keurentjes JC, Goeman JJ, Slagboom PE, Nelissen RG, Bos SD, Meulenbelt I. Genes involved in the osteoarthritis process identified through genome wide expression analysis in articular cartilage; the RAAK study. PLoS One 2014; 9: e103056.
[22] Li JH, Liu S, Zhou H, Qu LH and Yang JH. starbase v2.0: decoding miRNA-ceRNA, miRNA-ncRNA and protein–RNA interaction networks from large-scale CLIP-Seq data. Nucleic Acids Res 2014; 42: D92.
[23] Nahler G. Pearson correlation coefficient. Dictionary of Pharmaceutical Medicine 2009; 132-132.
[24] Best DJ and Roberts DE. Algorithm AS 89: the upper tail probabilities of spearman's rho. Applied Statistics 1975; 24: 377-379.
[25] Kanehisa M, Araki M, Goto S, Hattori M, Hirakawa M, Itoh M, Katayama T, Kawashima S, Okuda S and Tokimatsu T, Yamanishi Y. KEGG for linking genomes to life and the environment. Nucleic Acids Res 2008; 36: D480-484.
[26] Benjamini Y and Hochberg Y. Controlling the false discovery rate: a practical and powerful approach to multiple testing. Journal of the Royal Statistical Society. Series B (Methodological) 1995; 289-300.
[27] Li C, Han J, Yao Q, Zou C, Xu Y, Zhang C, Shang D, Zhou L, Zou C and Sun Z, Li J, Zhang Y, Yang H, Gao X, Li X. Subpathway-GM: identification of metabolic subpathways via joint power of interesting genes and metabolites and their topologies within pathways. Nucleic Acids Res 2013; 41: e101.
[28] Epstein MP, Duncan R, Jiang Y, Conneely KN, Allen AS and Satten GA. A permutation procedure to correct for confounders in case-control studies, including tests of rare variation. Am J Hum Genet 2012; 91: 215-223.
[29] Liang WC, Fu WM, Wong CW, Wang Y, Wang WM, Hu GX, Zhang L, Xiao LJ, Wan DC and Zhang JF, Waye MM. The lncRNA H19 promotes epithelial to mesenchymal transition by functioning as miRNA sponges in colorectal cancer. Oncotarget 2015; 6: 22513-22525.
[30] Bak RO and Mikkelsen JG. miRNA sponges: soaking up miRNAs for regulation of gene expression. Wiley Interdiscip Rev RNA 2014; 5: 317.
[31] Franke S, Sommer M, Rüster C, Bondeva T, Marticke J, Hofmann G, Hein G and Wolf G. Advanced glycation end products induce cell cycle arrest and proinflammatory changes in osteoarthritic fibroblast-like synovial cells. Arthritis Res Ther 2009; 11: R136.
[32] Sellam J, Berenbaum F. The role of synovitis in pathophysiology and clinical symptoms of osteoarthritis. Nat Rev Rheumatol 2010; 6: 625.
[33] Yang J and Wang N. Genome-wide expression and methylation profiles reveal candidate genes and biological processes underlying synovial inflammatory tissue of patients with osteoarthritis. Int J Rheum Dis 2015; 18: 783-790.
[34] Li X, Ye H, Yu F, Cai L, Li H, Chen J, Wu M, Chen W, Lin R and Li Z, Zheng C, Xu H, Wu G, Liu X. Millimeter wave treatment promotes chondrocyte proliferation via G1/S cell cycle transition. Int J Mol Med 2012; 29: 823-831.
[35] Kashiwagi A, Schipani E, Fein MJ, Greer PA and Shimada M. Targeted deletion of Capn4 in cells of the chondrocyte lineage impairs chondrocyte proliferation and differentiation. Mol Cell Biol 2010; 30: 2799-2810.
[36] Huang JG, Xia C, Zheng XP, Yi TT, Wang XY, Song G and Zhang B. 17β-Estradiol promotes cell proliferation in rat osteoarthritis model chondrocytes via PI3K/Akt pathway. Cell Mol Biol Lett 2011; 16: 564-575.
[37] Kang J, Chen W, Xia J, Li Y, Yang B, Chen B, Sun W, Song X, Xiang W, Wang X, Wang F, Bi Z, Wan

Y. Extracellular matrix secreted by senescent fibroblasts induced by UVB promotes cell proliferation in HaCaT cells through PI3K/AKT and ERK signaling pathways. Int J Mol Med 2008; 21: 777.

[38] Loeser RF, Goldring SR, Scanzello CR and Goldring MB. Osteoarthritis: a disease of the joint as an organ. Arthritis and rheumatism 2012; 64: 1697-1707.

[39] Issa RI and Griffin TM. Pathobiology of obesity and osteoarthritis: integrating biomechanics and inflammation. Pathobiol Aging Age Relat Dis 2012; 2.

[40] Chen J, Crawford R and Xiao Y. Vertical inhibition of the PI3K/Akt/mTOR pathway for the treatment of osteoarthritis. J Cell Biochem 2013; 114: 245.

[41] Børresen-Dale AL. TP53 and breast cancer. Hum Mutat 2003; 21: 292.

[42] Chiu TH, Lan KY, Yang MD, Lin JJ, Hsia TC, Wu CT, Yang JS, Chueh FS and Chung JG. Diallyl sulfide promotes cell-cycle arrest through the p53 expression and triggers induction of apoptosis via caspase- and mitochondria-dependent signaling pathways in human cervical cancer Ca Ski cells. Nutr Cancer 2013; 65: 505-514.

[43] Usmani SE, Pest MA, Kim G, Ohora SN, Qin L and Beier F. Transforming growth factor alpha controls the transition from hypertrophic cartilage to bone during endochondral bone growth. Bone 2012; 51: 131-141.

[44] Hall KC, Hill D, Otero M, Plumb DA, Froemel D, Dragomir CL, Maretzky T, Boskey A, Crawford HC and Selleri L, Goldring MB, Blobel CP. ADAM17 controls endochondral ossification by regulating terminal differentiation of chondrocytes. Mol Cell Biol 2013; 33: 3077.

[45] Zhang X, Zhu J, Li Y, Lin T, Siclari VA, Chandra A, Candela EM, Koyama E, Enomoto-iwamoto M and Qin L. Epidermal growth factor receptor (EGFR) signaling regulates epiphyseal cartilage development through β-catenin-dependent and -independent pathways. J Biol Chem 2013; 288: 32229-32240.

[46] Zintzaras E, Doxani C, Koufakis T, Kastanis A, Rodopoulou P and Karachalios T. Synopsis and meta-analysis of genetic association studies in osteoporosis for the focal adhesion family genes: the CUMAGAS-OSTEOporosis information system. BMC Med 2011; 9: 9.

[47] Mackenzie B and Erickson JD. Sodium-coupled neutral amino acid (System N/A) transporters of the SLC38 gene family. Pflugers Arch 2004; 447: 784.

[48] Chaudhry FA, Reimer RJ, Krizaj D, Barber D, Stormmathisen J, Copenhagen DR, Edwards RH. Molecular analysis of system N suggests novel physiological roles in nitrogen metabolism and synaptic transmission. Cell 1999; 99: 769-780.

[49] Nissenmeyer LSH and Chaudhry FA. Corrigendum: protein kinase C phosphorylates the system N glutamine transporter SN1 (Slc38a3) and regulates its membrane trafficking and degradation. Front Endocrinol (Lausanne) 2013; 4: 138.

[50] Reckziegel D, Raschke F, Cottam WJ and Auer DP. Cingulate GABA levels inversely correlate with the intensity of ongoing chronic knee osteoarthritis pain. Mol Pain 2016; 12.

Supplementary Table 1. Co-expressed lncRNA-mRNA interactions

LncRNAs	mRNAs	*P* value
TAPT1-AS1	C9orf142	0.020796
ZNF503-AS2	KCNMA1	0.007918
SNHG11	MRPL53	0.001061
FOXN3-AS1	PXMP2	0.018733
H1FX-AS1	WDR13	0.000287
LINC00476	ZFY	0.014779
SEMA3B	CDC14A	0.018772
UHRF1	FZD7	0.005294
UHRF1	MMP14	8.37E-05
UHRF1	TP53I3	0.008129
UBXN8	SHC1	0.022423
UBXN8	TCF7L1	0.020685
UBXN8	CCNE2	0.006498
PPP1R9B	CD44	0.014635
H19	PTEN	0.001873
SPON1	GLI1	0.015996
ZNF761	EGFR	0.027012
ZNF761	MCL1	0.031725
VPS11	CLOCK	0.002545
VPS11	FOXO1	0.030394
DCP1A	EGFR	0.005504
DCP1A	TP53	0.025784
LINC00476	MTOR	0.028292
LINC00521	NTRK3	0.006817
LINC00116	APP	0.002536
LINC00116	HSPB2	5.07E-05
CASC2	ATM	0.029099
LINC00174	RDX	0.049601
LINC00174	IRS1	0.029037
PCBP1-AS1	ACSL1	0.000486
PCBP1-AS1	SIRT1	0.005737
LINC00482	GLTSCR2	0.010638
LINC00482	GLTSCR2	0.010638
LINC00482	HNRNPU	0.016928
LINC00482	CSTF3	0.001814
LINC00482	ABCB7	0.003116
LINC00482	GNAT2	0.000449
LINC00482	ORC3	0.036621
LINC00482	NUP160	0.023165
LINC00482	UBR5	0.002775
LINC00482	PNN	0.014918
LINC00482	SYMPK	0.011208
LINC00482	POLR2I	0.019806
LINC00482	MCM5	0.037922
LINC00482	TPM2	0.008203
LINC00482	MCM2	1.95E-05
LINC00482	PPP2R5A	0.006401
LINC00482	EXOC3	0.005156
KTN1-AS1	TAB3	0.030462
LINC00265	H3F3B	0.014554
LINC00265	H3F3B	0.014554
LINC00265	CARD8	3.10E-05
LINC00265	MYB	0.001984
LINC00265	H3F3B	0.014554
LINC00265	PNN	0.023655
LINC00265	GTF2H1	0.001533
LINC00265	GOLPH3L	0.034189
LINC00265	CDK2	0.001312
SLC38A3	EP300	0.008672
SLC38A3	PKM	0.007572
SLC38A3	WASF3	0.005501
SLC38A3	TP53	0.033759
SLC38A3	SMO	0.000197
SLC38A3	EGFR	0.000199
LINC00319	ACVR2B	0.026085
CRYM-AS1	RBL2	0.004796
LINC00173	IL6R	8.89E-05
LINC00173	CYLD	0.011211
LINC00173	CREB1	1.49E-07
RNU12	PTK2B	0.000183
SNHG5	CDKN1C	0.043245
DGKK	IL24	0.010587
DGKK	TJP2	0.011003
MEG3	SRSF1	0.019223
MIR17HG	LEFTY1	0.000733
CROCCP2	CUL5	0.001541
CROCCP2	NOTCH2	9.51E-06
CROCCP2	SIRT1	0.001238
CROCCP2	BMPR2	0.011873
EPB41L4A-AS1	E2F3	0.004195
EPB41L4A-AS1	EGFR	0.000956
MIAT	TNFAIP3	0.020953
MIAT	COL1A1	0.034354
MIAT	CD276	0.029338
ZNF883	NLK	0.020342
ZNF883	BCL2	0.010237
ZNF883	IL2	0.008702
LINC00242	ITGA1	0.023556
LINC00242	EMD	0.004885
LINC00242	CLTC	0.006018
LINC00242	TPM3	0.015882
LINC00242	SRSF6	0.000157
LINC00242	UGGT1	0.002456
LINC00242	GNAS	0.031293
LINC00242	RPP40	0.000167

LINC00242	PQBP1	0.044638	TTTY15	NEFM	0.000284
LINC00242	CAMK2G	0.015456	MAGI2-AS3	FZD3	0.005842
LINC00242	CPSF1	1.30E-05	MAGI2-AS3	STAM2	0.028667
LINC00242	CSTF3	0.001131	MAGI2-AS3	LAMB3	0.003474
LINC00242	POLA2	0.000137	MAGI2-AS3	TIAM1	0.012739
LINC00242	ATP6V1E1	0.004121	JRK	IGF1R	0.002306
LINC00242	HNRNPA3	8.01E-05	JRK	RARA	0.000365
LINC00242	PRKAG1	0.000882	JRK	RPS6KA1	0.025538
LINC00242	XPOT	0.029639	MCF2L-AS1	PTK2	0.049984
LINC00242	UGGT2	0.030781	BCYRN1	SRSF2	0.005313
LINC00242	IQGAP3	0.012135	BCYRN1	SRSF2	0.005313
LINC00242	CPSF1	1.30E-05	MIR600HG	HES1	0.046238
LINC00242	CPSF1	1.30E-05	MIR600HG	ERBB2	0.044947
LINC00242	HNRNPA1L2	0.001433	LINC00312	TP53INP1	0.004705
LINC00242	MCM6	0.002328	LINC00312	BMPR2	0.015022
LINC00242	PARVA	0.022557	LINC00312	RBL2	0.003773
LINC00242	LNPEP	0.004744	DNAJC3-AS1	CCNT1	0.000541
LINC00242	AP3B1	0.014676	DNAJC3-AS1	CYP3A4	0.000895
LINC00242	PRKDC	9.34E-06	PVT1	WEE1	0.020413
LINC00242	AP1M1	0.001635	SCARNA9	P4HB	0.000112
LINC00242	MAP2K3	0.020865	C14orf169	ITGA2	0.009380
LINC00242	MAP2K3	0.020865	C14orf169	SLC38A1	0.037817
DLEU2	ARHGEF6	0.006329	RN7SL1	CYP8B1	0.003425
SNHG15	YWHAG	0.017051	ERVK13-1	CYCS	0.015019
SNHG15	TCF7L1	0.001231	FBXL19-AS1	TOB2	0.000997
LINC00472	LEFTY2	0.001207	FBXL19-AS1	GRB2	0.024463